Supplementary Information

(SI)

Is Nickel Phosphide an Efficient Catalyst for Oxygen-Evolution Reaction at Low Overpotentials?

Amirreza Valizadeh[a] and Mohammad Mahdi Najafpour*[a-c]

[a]Department of Chemistry, Institute for Advanced Studies in Basic Sciences (IASBS), Zanjan, 45137-66731, Iran

[b]Center of Climate Change and Global Warming, Institute for Advanced Studies in Basic Sciences (IASBS), Zanjan, 45137-66731, Iran

[c]Research Center for Basic Sciences & Modern Technologies (RBST), Institute for Advanced Studies in Basic Sciences (IASBS), Zanjan 45137-66731, Iran

*Corresponding author; Phone: (+98) 24 3315 3201; E-mail: mmnajafpour@iasbs.ac.ir

Table of contents

Materials

All reagents and solvents were obtained from commercial sources and used without further purification. Ni_2P, K_2FeO_4, and fluorine-doped tin oxide (FTO) were purchased from Sigma-Aldrich. Glassy carbon disk Working electrodes were purchased from CH Instruments. For the experiments, milli-Q water (18-20 MΩ•cm^{-1} at 27 °C) was used.

Methods

SEM was carried out using an LEO 1430VP microscope. HRTEM and TEM were carried out using an FEI Tecnai G^2 F20 transmission electron microscope, TF20 (200 kV). The X-ray powder diffraction patterns were recorded with a Bruker D8 Advance (Germany) diffractometer (CuK_α radiation). EDX analysis/mapping was carried out with the scanning electron microscope CamScan 4DV (CamScan UK). X-ray photoelectron spectroscopy (XPS, K-ALPHA, Thermo Scientific) was used to analyze the surface of the samples. All spectra were collected using Al-K radiation (1486.6 eV), monochromatized by a twin crystal monochromator, yielding a focused X-ray spot at 3 mA × 12 kV. The alpha hemispherical analyzer was operated in the constant energy mode with survey scan pass energies of 200 eV to measure the whole energy band, and with survey scan pass energies of 50 eV in a narrow scan to selectively measure the particular elements. XPS data were analyzed with Avantage software. A smart background function was used to approximate the experimental backgrounds and surface elemental composition was calculated from background-subtracted peak areas. Charge compensation was achieved with the system flood gun that provides low energy electrons and low energy argon ions from a single source. The penetration depth was around 3 nm.

Electrochemistry

Electrochemical experiments were performed using an $EmStat^{3+}$ from PalmSens (Netherlands). Cyclic voltammetry studies were carried out with a conventional three-electrode set-up, in which FTO (or GC), Hg|HgO and a platinum foil served as the working, reference, and auxiliary electrodes, respectively. Pt had no effect on the oxygen-evolution reaction of Ni/Fe oxide (see Figure S9). The result was not surprising, because the onset of Ni/Fe oxide was lower than Pt/Fe. All the potentials in this project were reported vs. RHE. The distance between two opposite sides of the FTO electrode was measured by a digital caliper MarCal 16ER model (Mahr, Germany). For Fe-free experiments, a polypropylene container was used instead of a standard cell. H_2SO_4 (6.0 M) in the polypropylene container was stirred for one hour and then carefully washed by water.

Electrode preparation

The commercial Ni_2P (4.0 mg) was dispersed as a mixture solution of H_2O (0.5 ml) and 5% Nafion (20 µl). A measure of the above suspension (50 µl) was drop-casted onto a pre-polished FTO electrode (1 cm^2), and dried at 50 °C for 30 min for the solvent to evaporate.

Conversion

A procedure introduced by Allen J. Bard was used to track the stability of Ni_2P under the electrochemical water-oxidation conditions [1]. In this method, the experiment was performed by a convective-suspension-collision technique, in which Ni_2P (100.0 mg) was suspended in an electrolyte (100 ml, KOH 1.0 M). It was continuously stirred such that the particles collided with a working electrode at ambient temperature at 1.79 V (V vs. RHE) for three days. The electrolyte was KOH (1.0 M), an Hg|HgO served as the reference electrode and a platinum sheet as an auxiliary electrode. Another platinum sheet was used as a working electrode. The experiment was performed using an HA-151 potentiostat-galvanostat (Hokuto Denko (Japan)). The set-up for the conversion procedure is shown in Scheme S2.

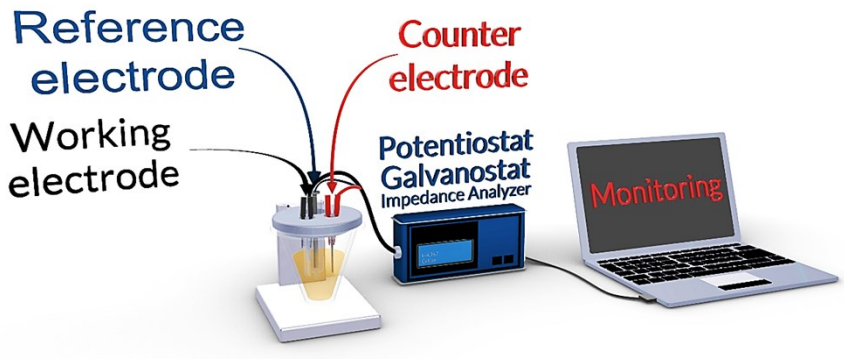

Scheme S1 Set-up for the electrochemical experiments.

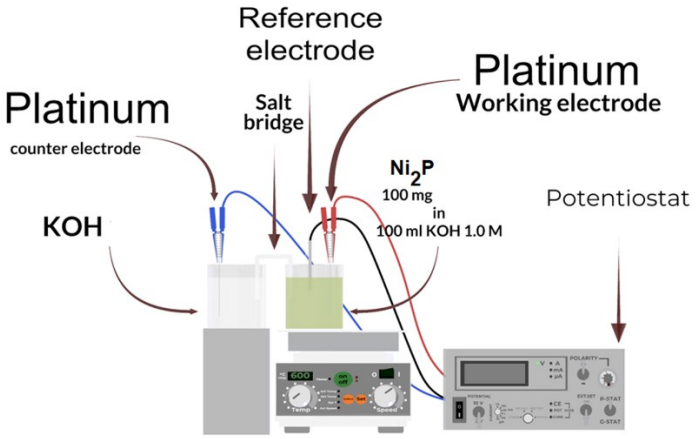

Scheme S2 Set-up for the conversion procedure. The set-up was used to obtain samples for HRTEM and NMR.

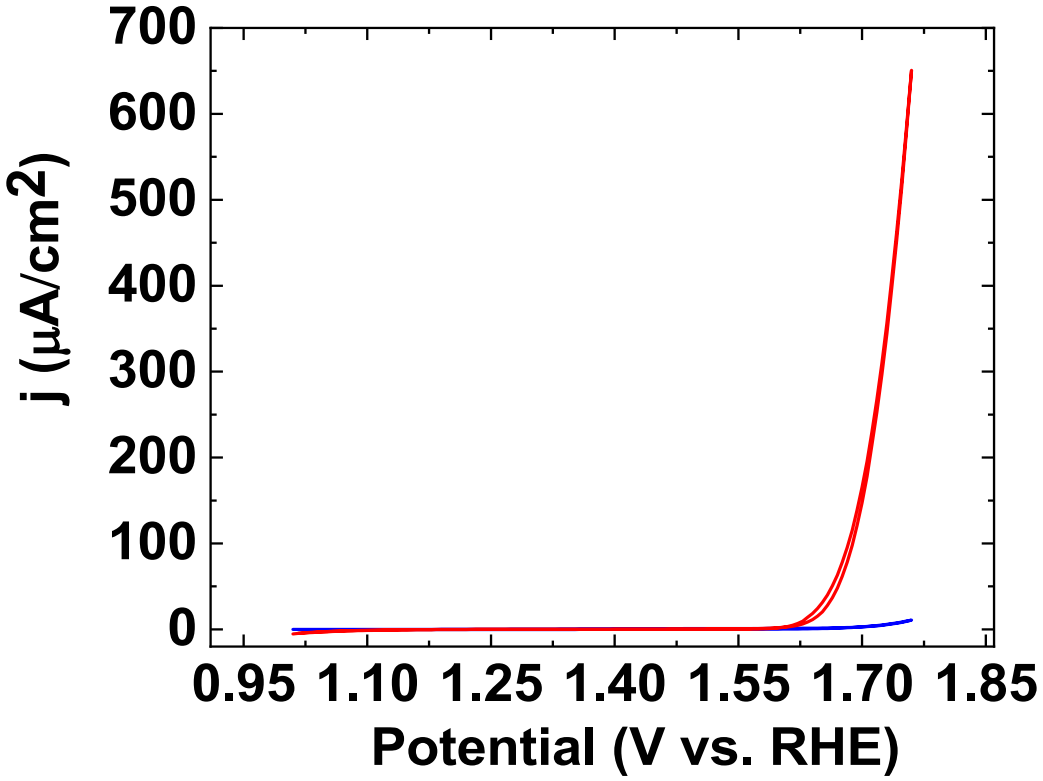

Figure S1 CVs for a bare FTO in KOH (0.10 M) before (blue) and after (red) adding Fe salt (scan rate: 100 mV/s).

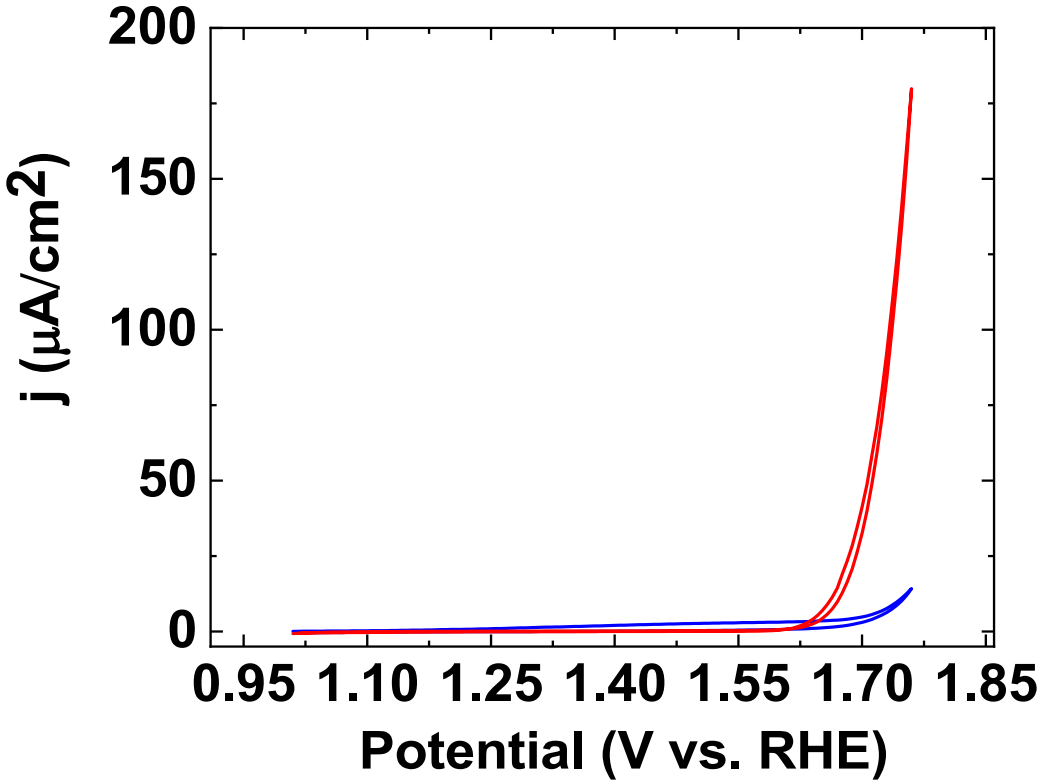

Figure S2 CVs for a bare FTO contains Nafion in KOH (0.10 M) before (blue) and after (red) adding Fe salt (scan rate: 100 mV/s).

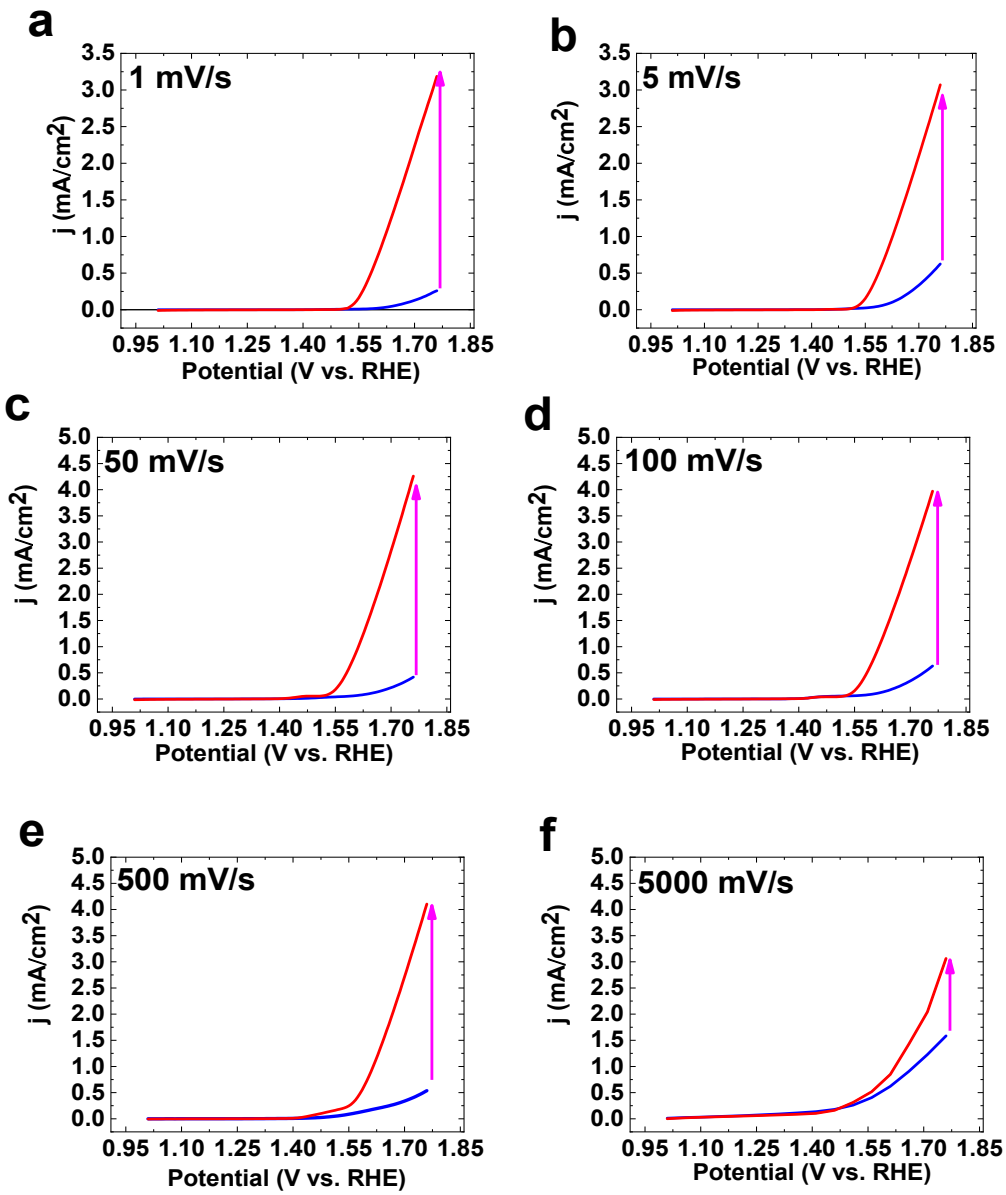

Figure S3 LSVs of Ni_2P in KOH (0.10 M) in the absence (blue) and the presence (red) of Fe salt at different scan rates.

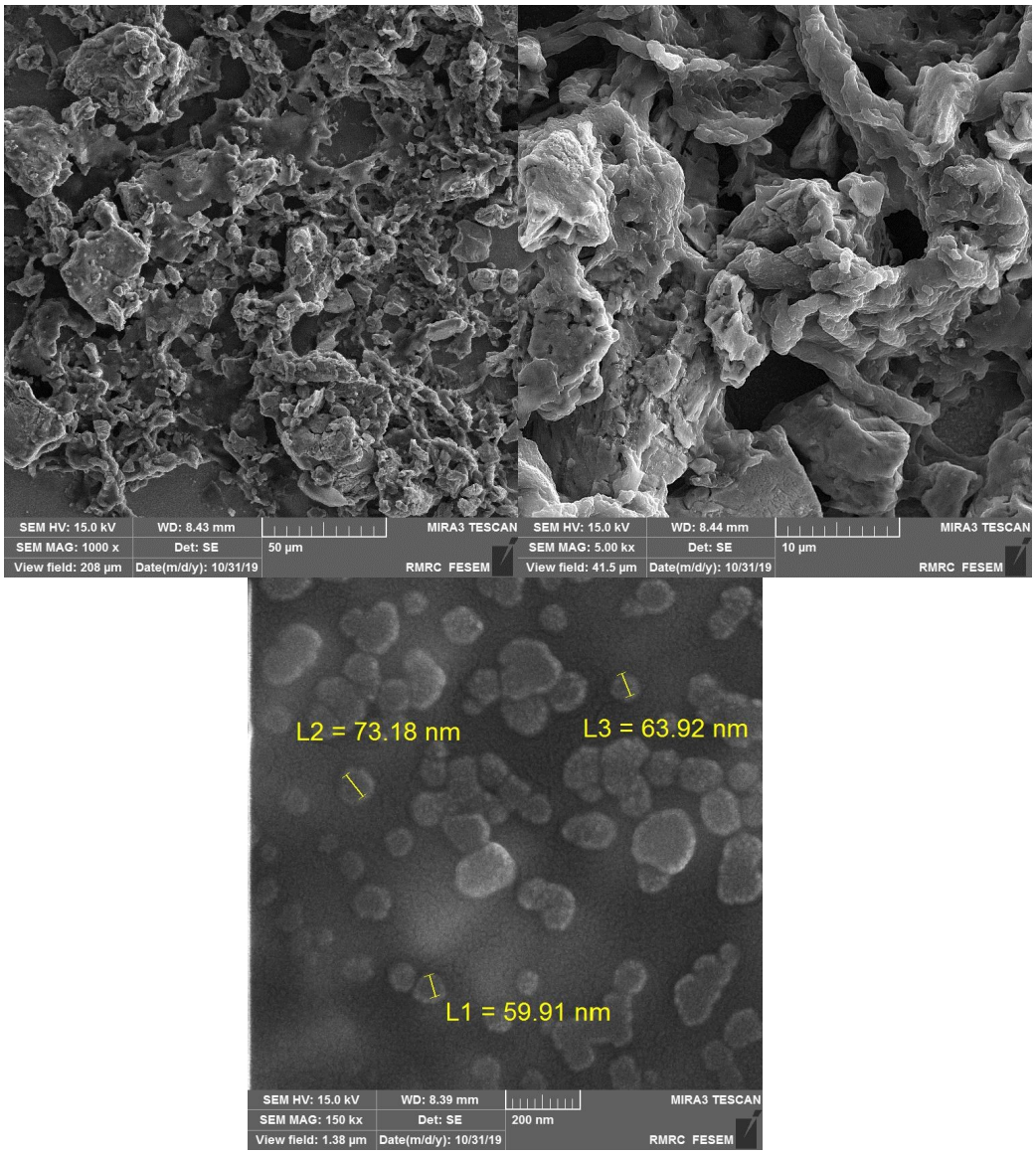

Figure S4 SEM images (at different magnifications) of the covered commercial Ni_2P on the surface of FTO by Nafion in the absence of potential.

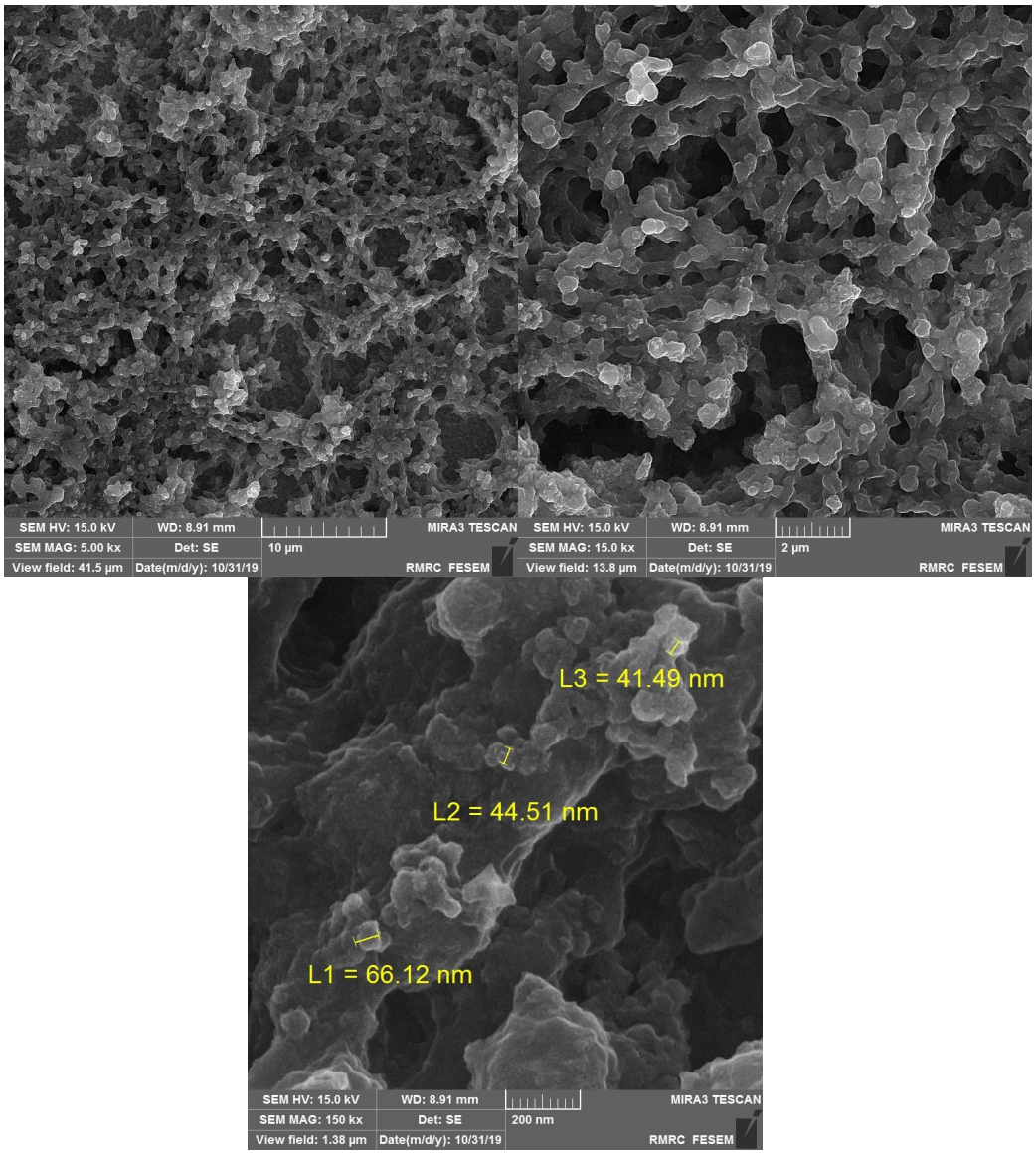

Figure S5 SEM images (at different magnifications) of the commercial Ni_2P on the surface of FTO after the consecutive 250 CVs in KOH (0.10 M): Range: 1.0-1.75V; scan rate: 100 mV/s.

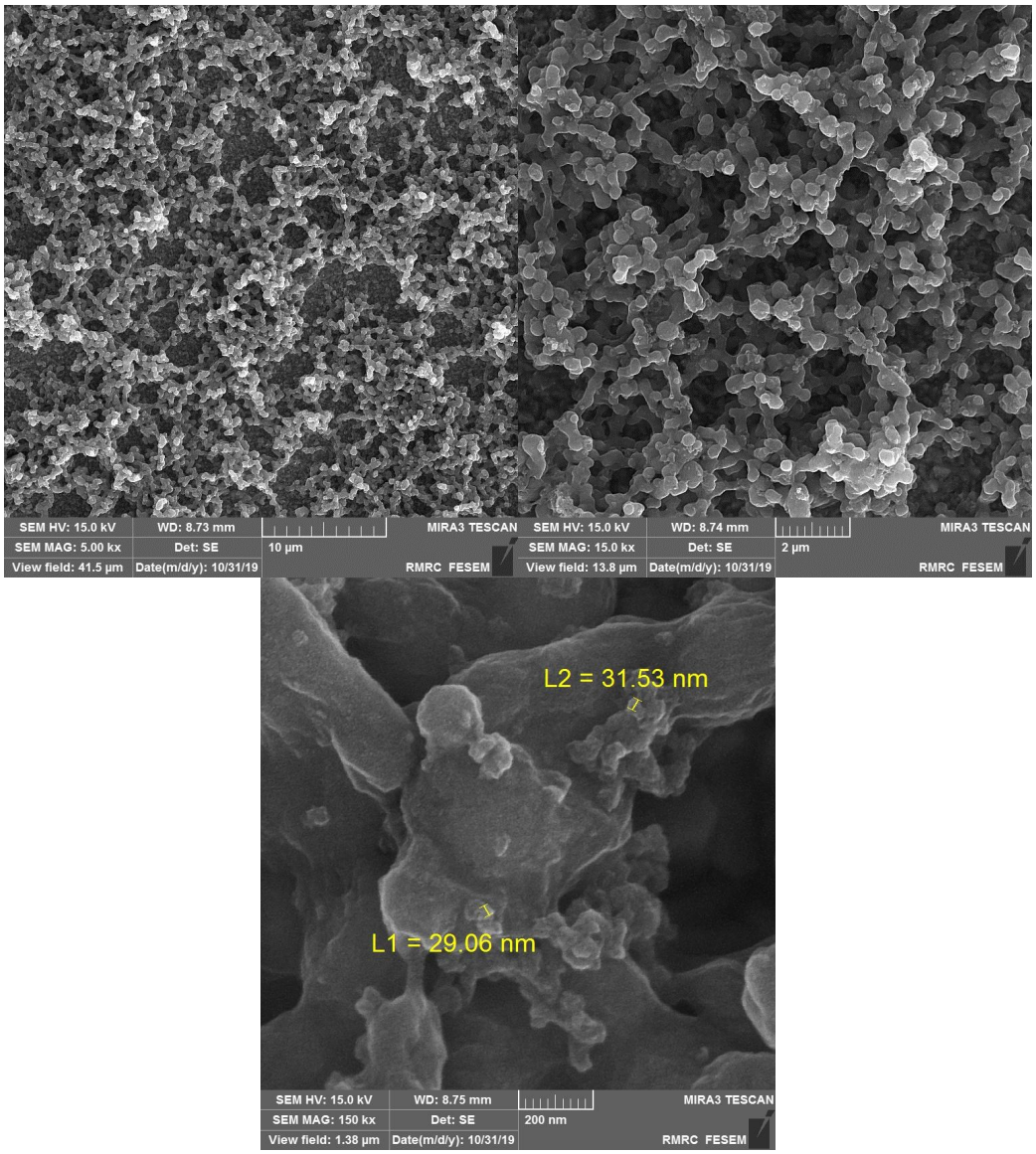

Figure S6 SEM images (at different magnifications) of the commercial Ni_2P on the surface of FTO after the consecutive 250 CVs in KOH (0.10 M) and then another 250 CVs in the presence of Fe salt. Range: 1.0-1.75V; scan rate: 100 mV/s.

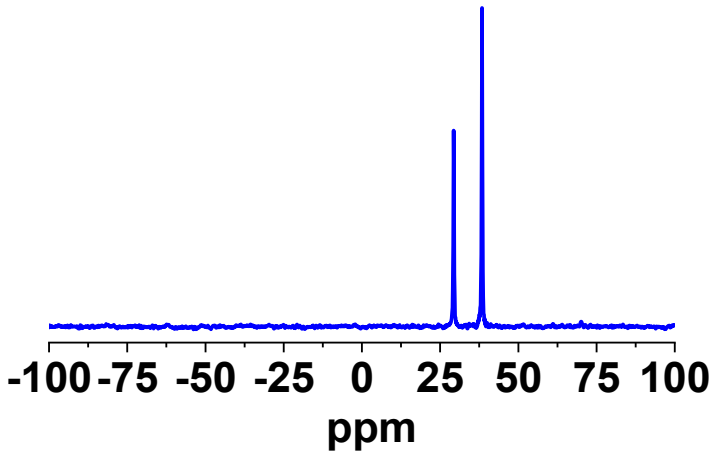

Figure S7 ^{31}P NMR of the commercial Ni_2P on the surface of Pt after the operation in KOH (1.0 M) (for the details of the preparation of sample, see Scheme S2).

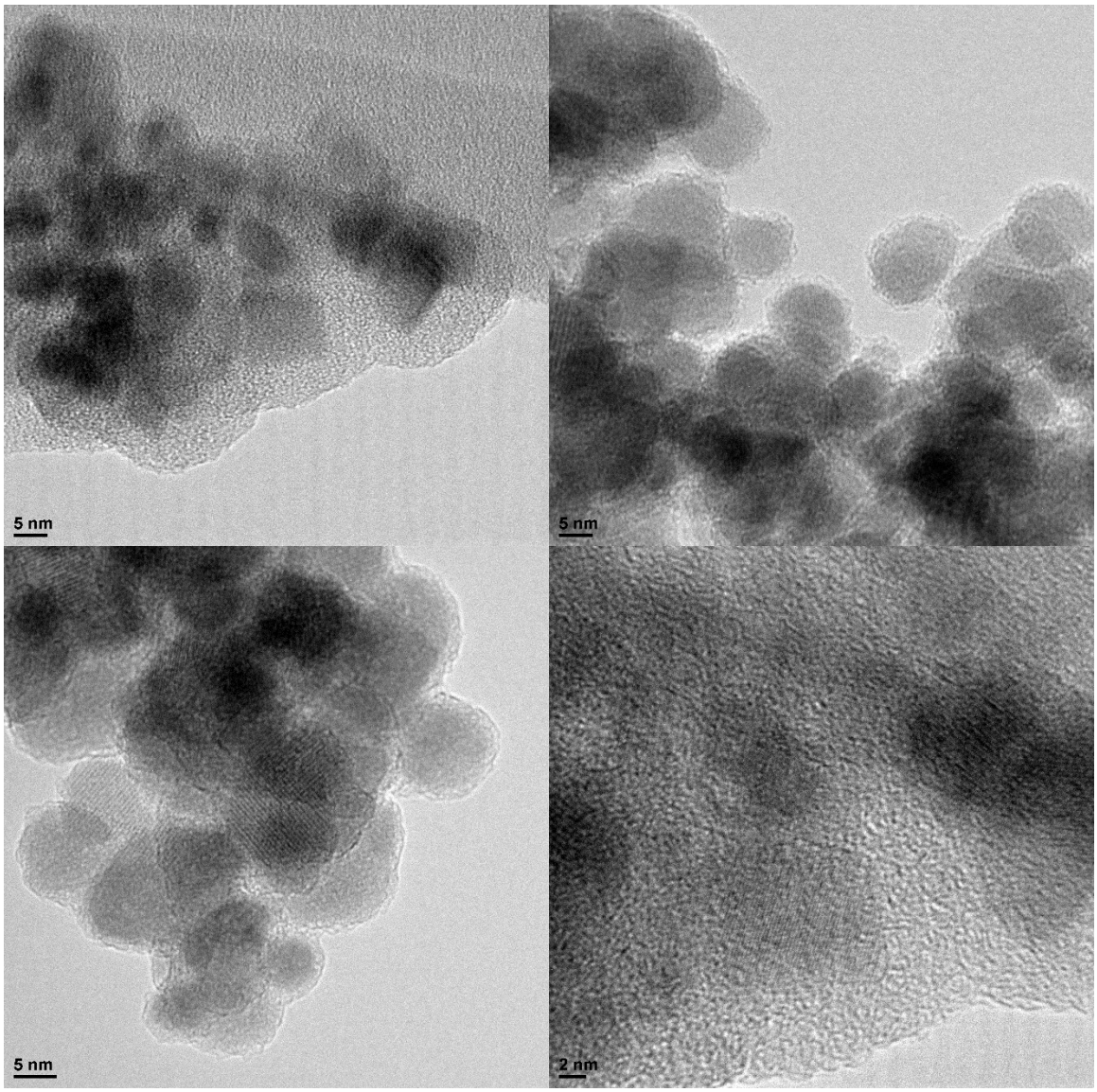

Figure S8 HRTEM images (at different magnifications) of the commercial Ni_2P on the surface of Pt after the operation in KOH (1.0 M) (for the details of the preparation of sample, see Scheme S2).

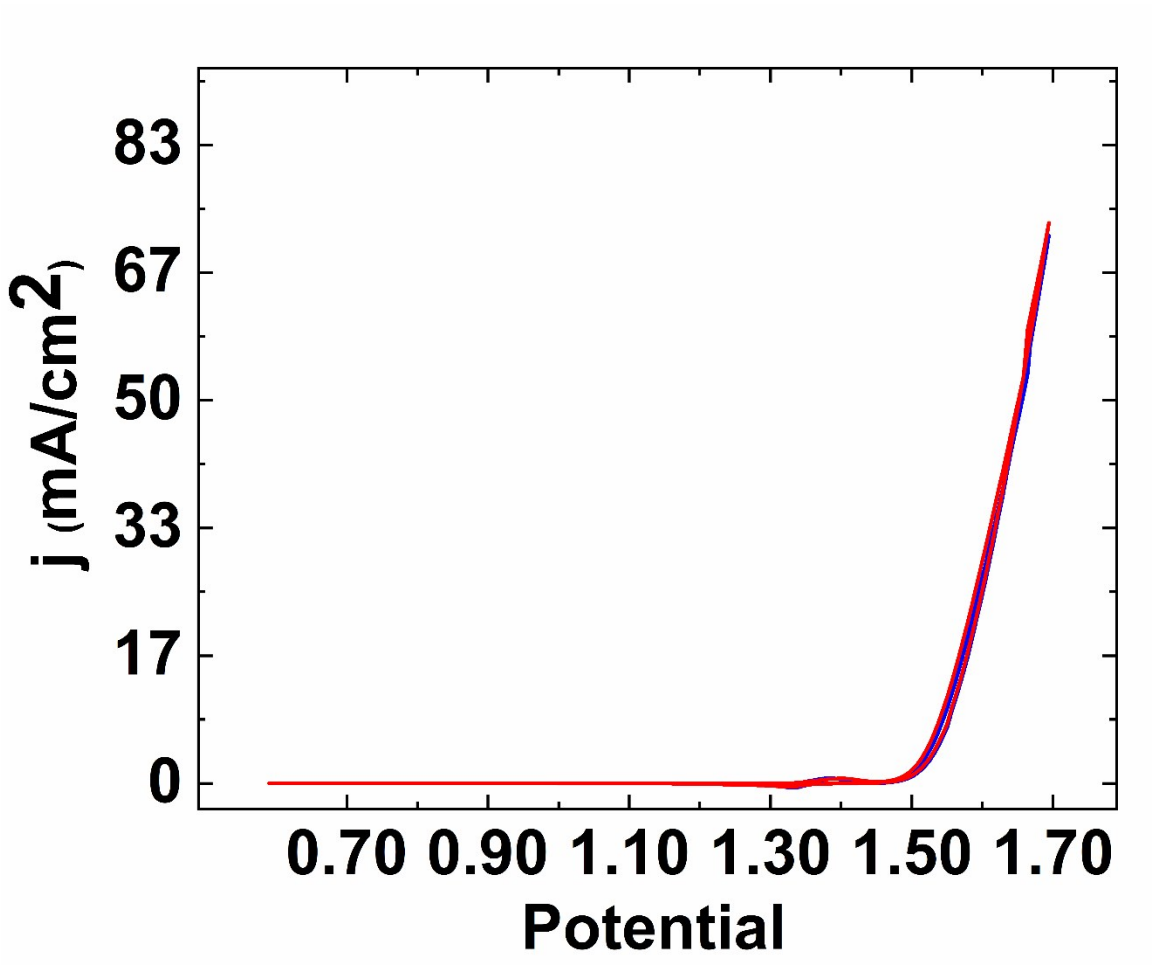

Figure S9 The effect of Pt salt (tetraammineplatinum(II) nitrate (99.995%, Sigma-Aldrich) on the OER of Ni oxide in the presence of Fe (saturated in the electrolyte) in a commercial KOH electrolyte solution (1.0 M). The blue and red CVs are related to Ni electrode in the absence (blue) and the presence of Pt salt (total concentration: 16 ppm) (red). The counter electrode was a graphite rod (diameter: 5.4 mm; length: 13 mm).

Table S1 Comparison of some heterogeneous water-oxidizing catalysts.

Compound	η[a] (mV)	η[b] (mV)	pH	Ref.[d]
$Ni_2P/NiO_x/Fe$	**217**	**287**	**13**	**This Work**
$NiFeO_x$	-	297	14	2
NiO_x	> 400	> 1000	14	3
NiO_x	-	300	14	2
CoO_x	-	381	14	2
$NiCoO_x$	-	312	14	2
FeO_x	345	445	14	4
FeO_x	-	405	14	2
Fe_2O_3	< 350	430	14	5
MnO_x	320	514	14	2
$Fe_3Ni_2O_x$	270	-	13	6
$FeNiO_x$	211	-	13	7
$Fe_2Ni_3O_x$	190	250	13	8
NiO_x	191	280	13	7
NiO_x	295	-	13	9
$CoFeO_x$[c]	397	-	13	10
CoO_x	< 200	< 250	13	11
FeO_x	320	410	13	7
CoO_x	210	270	13	7
CoO_x	295	-	13	6
$FeCoO_x$	181	-	13	7
$FeCoNiO_x$	191	-	13	7
Ni_2FeAlO_x	270	-	13	6
$NiFeMo_3O_x$	250	-	13	6
$Ni_2FeCr_2O_x$	240	-	13	6
$NiFeGa_3O_x$	240	-	13	6
$CoSe_2$	373	380	13	12
NG-$CoSe_2$	294	320	13	12
MnO_x	< 300	> 1000	>11.5	13
FeOOH	300	420	11	14
NiB_i	300	425	9.2	15
MnO_x	< 300	> 1000	8.5-5.5	13
CoO_x	< 200	< 300	7	11
MnO_x	390	590	7	16
MnO_x	441	600	7	17
CoFePBA	291	> 600	7	18
MnO_x	150	> 1000	7	19
CoP_i	281	410	7	20
MnO_x	> 700	> 1000	7	21
$Li_xMnP_2O_7$	500	-	7	22
MnO_x	< 300	> 1000	3.5	13
Co^{2+} (1 M)	< 580	600	1	11

[a] Onset overpotentiol.
[b] @1 $mAcm^{-2}$.
[c] LDH.
[d] For an excellent review, see ref. 23

References

1. X. Xiao and A. J. Bard*, J. Am. Chem. Soc*., 2007, **129**, 9610-9612.

2. Trotochaud, L.; Ranney, J. K.; Williams, K. N.; Boettcher, S. W., Solution-cast metal oxide thin film electrocatalysts for oxygen evolution. *J. Am. Chem. Soc.,* **2012**, *134* (41), 17253-17261.

3. Trotochaud, L.; Young, S. L.; Ranney, J. K.; Boettcher, S. W., Nickel-iron oxyhydroxide oxygen-evolution electrocatalysts: the role of intentional and incidental iron incorporation. *J. Am. Chem. Soc.,* **2014,** *136* (18), 6744-6753.

4. Doyle, R.; Lyons, M., Kinetics and mechanistic aspects of the oxygen evolution reaction at hydrous iron oxide films in base. *J. Electrochem. Soc.,* **2013**, *160* (2), H142-H154.

5. Qiu, Y.; Leung, S.-F.; Zhang, Q.; Hua, B.; Lin, Q.; Wei, Z.; Tsui, K.-H.; Zhang, Y.; Yang, S.; Fan, Z., Efficient photoelectrochemical water splitting with ultrathin films of hematite on three-dimensional nanophotonic structures. *Nano lett.,* **2014**, *14* (4), 2123-2129.

6. Chen, J. Y.; Miller, J. T.; Gerken, J. B.; Stahl, S. S., Inverse spinel $NiFeAlO_4$ as a highly active oxygen evolution electrocatalyst: promotion of activity by a redox-inert metal ion. *Energy Environ. Sci.,* **2014,** *7* (4), 1382-1386.

7. Smith, R. D.; Prévot, M. S.; Fagan, R. D.; Zhang, Z.; Sedach, P. A.; Siu, M. K. J.; Trudel, S.; Berlinguette, C. P., Photochemical route for accessing amorphous metal oxide materials for water oxidation catalysis. *Science,* **2013**, 1233638.

8. Smith, R. D.; Prévot, M. S.; Fagan, R. D.; Trudel, S.; Berlinguette, C. P., Water oxidation catalysis: electrocatalytic response to metal stoichiometry in amorphous metal oxide films containing iron, cobalt, and nickel. *J. Am. Chem. Soc.,* **2013**, *135* (31), 11580-11586.

9. Shaidarova, L.; Davletshina, L.; Budnikov, G., Flow-injection determination of water-soluble vitamins B 1, B 2, and B 6 from the electrocatalytic response of a graphite electrode modified with a ruthenium (III) hexacyanoruthenate (II) film. *J. Anal. Chem.,* **2006**, *61* (5), 502-509.

10. Abellán, G.; Carrasco, J. A.; Coronado, E.; Romero, J.; Varela, M., Alkoxide-intercalated CoFe-layered double hydroxides as precursors of colloidal nanosheet suspensions: structural, magnetic and electrochemical properties. *J. Mater. Chem. C,* **2014**, *2* (19), 3723-3731.

11. Gerken, J. B.; McAlpin, J. G.; Chen, J. Y.; Rigsby, M. L.; Casey, W. H.; Britt, R. D.; Stahl, S. S., Electrochemical water oxidation with cobalt-based electrocatalysts from pH 0–14: the thermodynamic basis for catalyst structure, stability, and activity. *J. Am. Chem. Soc.,* **2011**, *133* (36), 14431-14442.

12. Gao, M.-R.; Cao, X.; Gao, Q.; Xu, Y.-F.; Zheng, Y.-R.; Jiang, J.; Yu, S.-H., Nitrogen-doped graphene supported $CoSe_2$ nanobelt composite catalyst for efficient water oxidation. *ACS Nano* **2014**, *8* (4), 3970-3978.

13. Huynh, M.; Bediako, D. K.; Nocera, D. G., A functionally stable manganese oxide oxygen evolution catalyst in acid. *J. Am. Chem. Soc.,* **2014**, *136* (16), 6002-6010.

14. Chemelewski, W. D.; Lee, H.-C.; Lin, J.-F.; Bard, A. J.; Mullins, C. B., Amorphous FeOOH oxygen evolution reaction catalyst for photoelectrochemical water splitting. *J. Am. Chem. Soc.,* **2014**, *136* (7), 2843-2850.

15. Dincă, M.; Surendranath, Y.; Nocera, D. G., Nickel-borate oxygen-evolving catalyst that functions under benign conditions. *Proc. Natl. Acad. Sci.,* **2010**, *107* (23), 10337-10341.

16. Zaharieva, I.; Chernev, P.; Risch, M.; Klingan, K.; Kohlhoff, M.; Fischer, A.; Dau, H., Electrosynthesis, functional, and structural characterization of a water-oxidizing manganese oxide. *Energy Environ. Sci.,* **2012**, *5* (5), 7081-7089.

17. Indra, A.; Menezes, P. W.; Zaharieva, I.; Baktash, E.; Pfrommer, J.; Schwarze, M.; Dau, H.; Driess, M., Active Mixed-Valent MnOx Water Oxidation Catalysts through Partial Oxidation (Corrosion) of Nanostructured MnO Particles. *Angew. Chem. Int. Ed.,* **2013**, *52* (50), 13206-13210.

18. Pintado, S.; Goberna-Ferrón, S.; Escudero-Adán, E. C.; Galán-Mascarós, J. R. n., Fast and persistent electrocatalytic water oxidation by Co-Fe Prussian blue coordination polymers. *J. Am. Chem. Soc.,* **2013**, *135* (36), 13270-13273.
19. Singh, A.; Hocking, R. K.; Chang, S. L.-Y.; George, B. M.; Fehr, M.; Lips, K.; Schnegg, A.; Spiccia, L., Water oxidation catalysis by nanoparticulate manganese oxide thin films: probing the effect of the manganese precursors. *Chem. Mater.,* **2013**, *25* (7), 1098-1108.
20. Kanan, M. W.; Nocera, D. G., In situ formation of an oxygen-evolving catalyst in neutral water containing phosphate and Co^{2+}. *Science*, **2008**, *321* (5892), 1072-1075.
21. Bergmann, A.; Zaharieva, I.; Dau, H.; Strasser, P., Electrochemical water splitting by layered and 3D cross-linked manganese oxides: correlating structural motifs and catalytic activity. *Energy Environ. Sci.*, **2013**, *6* (9), 2745-2755.
22. Park, J.; Kim, H.; Jin, K.; Lee, B. J.; Park, Y.-S.; Kim, H.; Park, I.; Yang, K. D.; Jeong, H.-Y.; Kim, J., A new water oxidation catalyst: lithium manganese pyrophosphate with tunable Mn valency. *J. Am. Chem. Soc.,* **2014**, *136* (11), 4201-4211.
23 Galan-Mascarós, J. R., Water oxidation at electrodes modified with earth-abundant transition-metal catalysts. *ChemElectroChem*, **2015**, 2 (1), 37-50.